Current Biology 16, 359–370, February 21, 2006 ©2006 Elsevier Ltd All rights reserved DOI 10.1016/j.cub.2005.12.043

Article

Rho-kinase Controls Cell Shape Changes during Cytokinesis

Gilles R.X. Hickson,[1] Arnaud Echard,[2] and Patrick H. O'Farrell[1,*]

[1] Department of Biochemistry and Biophysics
University of California, San Francisco
San Francisco, California 94143-2200

[2] Institut Curie
Centre Nationale de la Recherche Scientifique
Unité Mixte de Recherche 144
75248 Paris Cedex 5
France

Summary

Background: Animal cell cytokinesis is characterized by a sequence of dramatic cortical rearrangements. How these are coordinated and coupled with mitosis is largely unknown. To explore the initiation of cytokinesis, we focused on the earliest cell shape change, cell elongation, which occurs during anaphase B and prior to cytokinetic furrowing.

Results: Using RNAi and live video microscopy in *Drosophila* S2 cells, we implicate Rho-kinase (Rok) and myosin II in anaphase cell elongation. *rok* RNAi decreased equatorial myosin II recruitment, prevented cell elongation, and caused a remarkable spindle defect where the spindle poles collided with an unyielding cell cortex and the interpolar microtubules buckled outward as they continued to extend. Disruption of the actin cytoskeleton with Latrunculin A, which abolishes cortical rigidity, suppressed the spindle defect. *rok* RNAi also affected furrowing, which was delayed and slowed, sometimes distorted, and in severe cases blocked altogether. Co-depletion of the myosin binding subunit (Mbs) of myosin phosphatase, an antagonist of myosin II activation, only partially suppressed the cell-elongation defect and the furrowing delay, but prevented cytokinesis failures induced by prolonged *rok* RNAi. The marked sensitivity of cell elongation to Rok depletion was highlighted by RNAi to other genes in the Rho pathway, such as *pebble*, *racGAP50C*, and *diaphanous*, which had profound effects on furrowing but lesser effects on elongation.

Conclusions: We show that cortical changes underlying cell elongation are more sensitive to depletion of Rok and myosin II, in comparison to other regulators of cytokinesis, and suggest that a distinct regulatory pathway promotes cell elongation.

Introduction

Cytokinesis and mitosis are temporally coordinated such that furrow ingression closely follows the segregation of sister chromosomes in anaphase. This coordination appears to be controlled by mitotic cyclins. Although the events coupling cytokinesis to cyclin destruction have not been fully elucidated, two essential cytokinetic functions appear to be regulated by cyclins: The function of the Rho-GEF encoded by *pebble* is limited by cyclins, and activity of a conserved mitotic kinesin-like protein is inhibited by cyclin/Cdk phosphorylation [1, 2]. The recruitment of myosin II to the cell equator, the assembly of the contractile ring, and activation of its contraction are also key events in the furrowing of the cell. Although several activities have been identified as contributing to these events (reviewed in [3–5], see below for pertinent examples), it is not clear how these apparently parallel inputs are coordinated with one another and how they may time the initiation of furrowing or control its progression.

In an effort to define the regulatory inputs that might convey the temporal control of cytokinesis, we have used RNAi to suppress the function of different regulators of cytokinesis in *Drosophila* S2 cells, a strategy that has already yielded much information [6–8]. Using real-time video microscopy to examine the ensuing phenotypic consequences, we have focused on the earliest events in the progress toward cytokinesis. When small cells such as tissue-culture cells enter mitosis, they generally adopt a spherical shape and resist experimental distortion through increased cortical rigidity [9, 10]. In anaphase, these spherical cells elongate and become capsule shaped as the anaphase spindle extends and the cells prepare for cytokinesis. Our focus has led us to characterize this process of anaphase cell elongation. Although the phenomenon has been appreciated for over a century, the relative contributions of equatorial contraction, polar relaxation, and spindle pushing forces are still to be resolved. Nor is it clear whether cell elongation simply reflects the earliest phase of the progression toward furrowing, or whether it involves distinct processes.

In *Drosophila*, the activity of the Rho guanine-nucleotide exchange factor, Pebble, is one input that contributes to the time of onset of furrowing [1, 11], but how it mediates temporal control is not clear. Pebble activation of Rho has two well-recognized types of inputs into the formation and function of the contractile ring. GTP-bound Rho interacts with Diaphanous, a formin that is essential for cytokinesis [12] and that nucleates unbranched actin filaments. GTP-bound Rho also promotes activation of myosin II, although there are at least two candidate effector kinases that might mediate myosin activation in cytokinesis: Rho-kinase (Rok) and Citron-kinase. Both of these are activated by Rho-GTP and have the potential to phosphorylate the myosin regulatory light chains (MRLCs) and hence activate myosin II ([13–15] reviewed in [16]), but various reports of their contributions are not in full accord. One report recently suggested that Citron-kinase plays the key role in mediating furrowing in *Drosophila* [17]. Conversely, our analysis of the phenotype resulting from RNAi suppression in S2 cells suggested that Citron-kinase was specifically

*Correspondence: ofarrell@cgl.ucsf.edu

required at a later step to stabilize the intercellular bridge that persists long after contractile ring function [6], a finding consistent with the failure of other investigators to define a furrowing defect in cells deficient in Citron-kinase [18, 19]. The other candidate kinase, Rok, has a second potential input into the activation of myosin II: It phosphorylates the myosin binding subunit of myosin phosphatase and inhibits it, an action that prevents the inactivation of myosin II [20].

We have found that RNAi-induced suppression of some but not all genes involved in furrowing blocks or delays anaphase cell elongation. In particular, we implicate Rok and myosin II in this event.

Results

Drosophila S2 Cells Elongate in Anaphase in Preparation for Cytokinesis

Using real-time video microscopy of *Drosophila* S2 cells expressing histone H2B-GFP, we monitored cells as they exited mitosis and progressed toward cytokinesis. An approximately 1.5-fold elongation of the cell in anaphase preceded and accompanied furrow formation. Toward the end of the elongation process, we frequently observed blebbing of the plasma membrane in the polar regions (90% of cells, $n > 10$, Figure 1A). These blebs expanded rapidly (within 15 s), establishing new boundaries at the leading edge of the elongating cells (Figure 1A and Movie 1 in the Supplemental Data available online); the membrane appeared to respond to and evade the oncoming spindle poles (Figure 1A and Movie 1). Such "polar blebbing," which was first detailed as early as 1883, might reflect alterations in the rigidity of the polar cortex (see [21, 22]). In addition to apparent relaxation of the polar cortex, myosin II becomes diffusely localized in the equatorial cortex (see below), where it might contribute to cell elongation through a broad equatorial contraction prior to the more focal contraction of the contractile ring driving furrow ingression.

Rho-kinase Is Essential for Anaphase Cell Elongation

In addition to a slowing of cytokinesis (see below), the normal extent of cell elongation was substantially reduced in cells treated for 2–3 days with double-stranded RNAs (dsRNAs) targeting *rok*. After an apparently normal metaphase-to-anaphase transition, the segregation of DNA masses stalled with the DNA in tight juxtaposition with the cell margin; the cortex was slightly distorted over the position of the DNA masses, and the live recordings suggested a forceful collision with a minimally compliant cortex (Figure 1B and Movie 2). Similarly, in fixed preparations, the DNA masses of late-anaphase and telophase cells following *rok* RNAi were much closer together than following a normal mitotic separation, the cells were still round, and staining for tubulin revealed a disrupted anaphase spindle that had not extended normally (Figure 1C). These phenotypes appear to be specific because they were seen with two nonoverlapping independent dsRNAs specific for *rok* and were not seen when cells were treated with control dsRNAs or in cells treated with dsRNAs that knock down other cytokinesis functions (see below). We conclude that Rok is specifically required in anaphase for elongation.

To monitor spindle dynamics in real time, we turned to an S2 cell line expressing GFP-tubulin [23]. In control cells undergoing anaphase, the array of interpolar MTs gathered centrally toward the spindle axis and lengthened parallel to this axis (Figure 1D and Movie 3). The central spindle, an important component of the cytokinetic machinery [3–5], developed amid this array of interpolar fibers. Following *rok* RNAi, all appeared normal during anaphase A, but, as anaphase B began, the separating spindle poles collided with the cortex, and the interpolar MTs buckled outward with the inflection point located at the midpoint of the spindle. During what would ordinarily be anaphase B, the interpolar MTs continued to extend, thereby exaggerating the buckling (Figures 1E and 1F and Movies 4 and 5). Measuring the length of the MTs during normal anaphase B (essentially the pole-to-pole distance) and the length of the buckled MTs in the *rok*-RNAi-treated cells (measured from one pole to the inflection and then back to the other pole) suggested that the MTs elongated to the same extent in the undisturbed cells and in the RNAi-depleted cells (Figure 2A). At the onset of buckling, when the interpolar MTs were parallel to the long axis of the spindle, small bulges in the cell cortex overlaid the spindle poles, suggesting a force of extension along the spindle. However, these bulges diminished as the inflection point of the MTs moved out toward the equatorial cortex and the angle between the MTs and the spindle axis increased. Such an altered spindle configuration would be predicted to shift the direction of force generated by the elongating MTs from one that is parallel to the spindle axis to one that is increasingly perpendicular to the spindle. Accordingly, some cells would actually expand at the equator, becoming oval in shape with the poles of the spindle aligned with the short axis (Figure 1C, center). Although furrowing was substantially delayed and slowed (described below), many cells went on to successfully complete cytokinesis despite pronounced defects in cell elongation.

The early *rok* RNAi phenotype led us to hypothesize that the spindle suffered a mechanical collapse when it continued to elongate within a cell whose cortex was unyielding and would no longer accommodate the elongating spindle. Because the spindle continued to extend and appeared capable of exerting force, it might be able to elongate the cell if the rigidity of the cortex were suppressed. Latrunculin A (LatA) prevents actin polymerization and thereby reduces cortical rigidity [24, 25]. In the presence of 1 μg/ml LatA, control S2 cells were round in metaphase and then elongated 1.5-fold in anaphase (Figures 2B and 2C). The early stages of spindle extension were not perturbed by LatA treatment. However, polar blebbing was not observed, and the cell cortex appeared to have lost rigidity because it passively adopted the pointed shape of the spindle as it elongated (Movie 6). Cytokinetic furrows failed to form, as expected, and the central-spindle structure failed to fully compact and instead lost integrity. In contrast to *rok* RNAi in the absence of LatA, *rok*-dsRNA-treated cells elongated when in the presence of LatA (Figure 2D). Indeed, these cells were indistinguishable from control LatA-treated cells (Figure 2 and Movies 6 and 7).

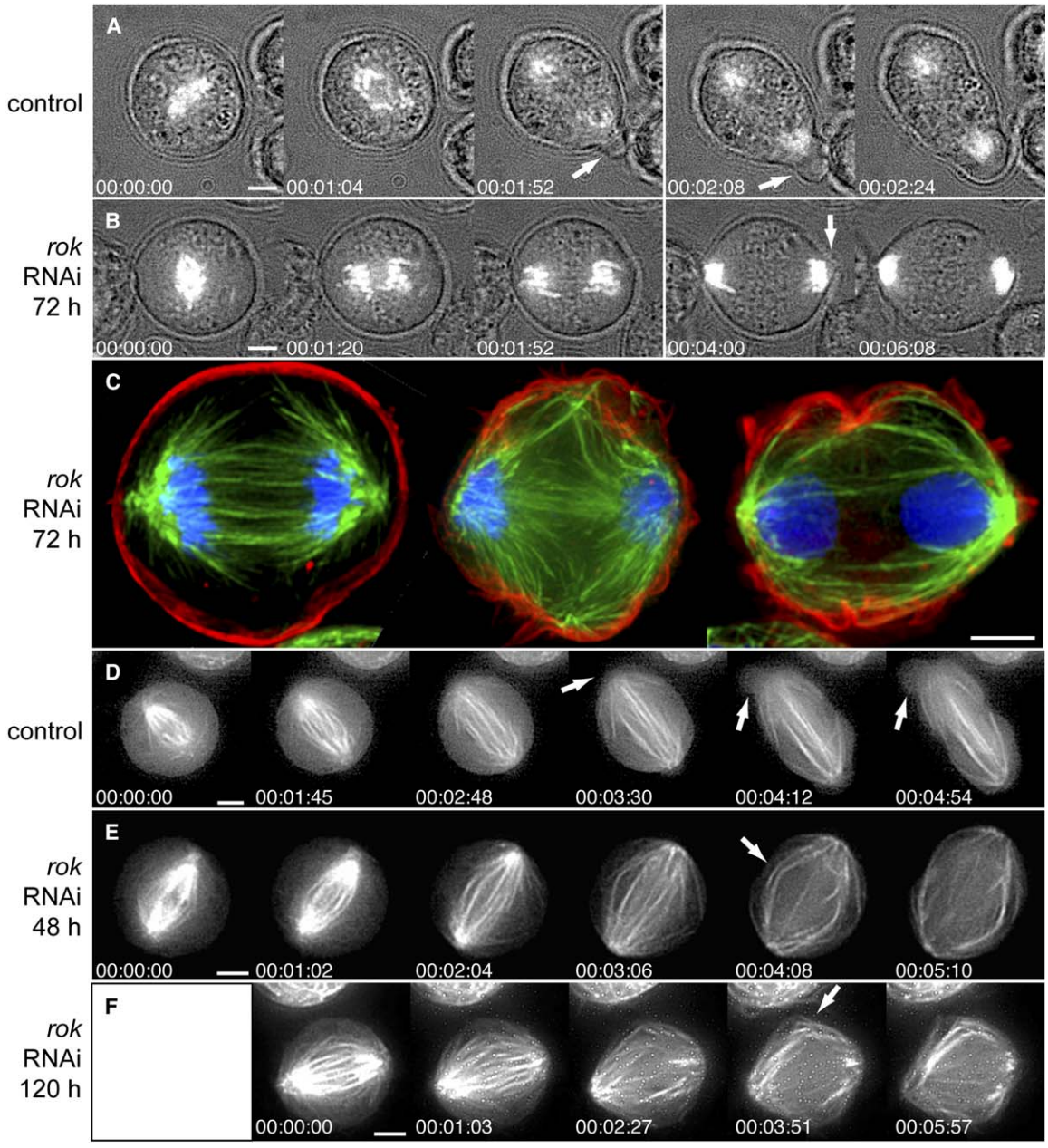

Figure 1. Rho-kinase Is Required for Anaphase Cell Elongation

(A–B) Selected frames from time-lapse sequences of *Drosophila* S2 cells, stably expressing histone H2B-GFP, progressing through anaphase (time from the metaphase/anaphase transition indicated in hr:min:s). (A) A typical control cell undergoing anaphase cell elongation. Note the appearance of a polar bleb (arrows: 00:01:52, 00:02:08), allowing for the establishment of a new cell boundary to accommodate the segregating DNA masses (00:02:24; see also Movie 1). (B) A cell following 72 hr *rok* RNAi failed to elongate in anaphase. No polar blebs appeared, and the spindle poles and segregating DNA masses smashed up against the cell cortex, which bulged slightly outward (arrow). Although furrow ingression was delayed and did not initiate within the 6 min of the sequence depicted here, the cell ultimately divided successfully (see Movie 2).
(C) Fixed images of S2 cells following 72 hr *rok* RNAi, stained for DNA (blue), MTs (green), and F-actin (red). Whereas the cell in late anaphase A (left) appears normal, the anaphase B cell (middle) and telophase cell (right) have failed to elongate. Note the buckled appearance of the MTs in the middle panel.
(D–F) Selected frames from fluorescent time-lapse sequences of GFP-tubulin expressing S2 cells in anaphase. (D) A typical control cell. As the cell and spindle coordinately elongated in anaphase, polar blebs appeared (arrows), and the centrally localized interpolar MTs elongated parallel to the spindle axis (00:03:30-00:04:54, see Movie 3). (E) A cell following 48 hr rok RNAi. As the separating spindle poles reached the cell cortex, no polar blebs were observed, cell elongation did not keep pace with spindle extension, and the interpolar MTs buckled outwards (arrow, 00:04:08, see Movie 4). (F) A cell following 120 hr *rok* RNAi. Again, the interpolar MTs buckled outward in the absence of cell elongation (arrow, 00:03:51, see Movie 5). Scale bars represent 3 μm.

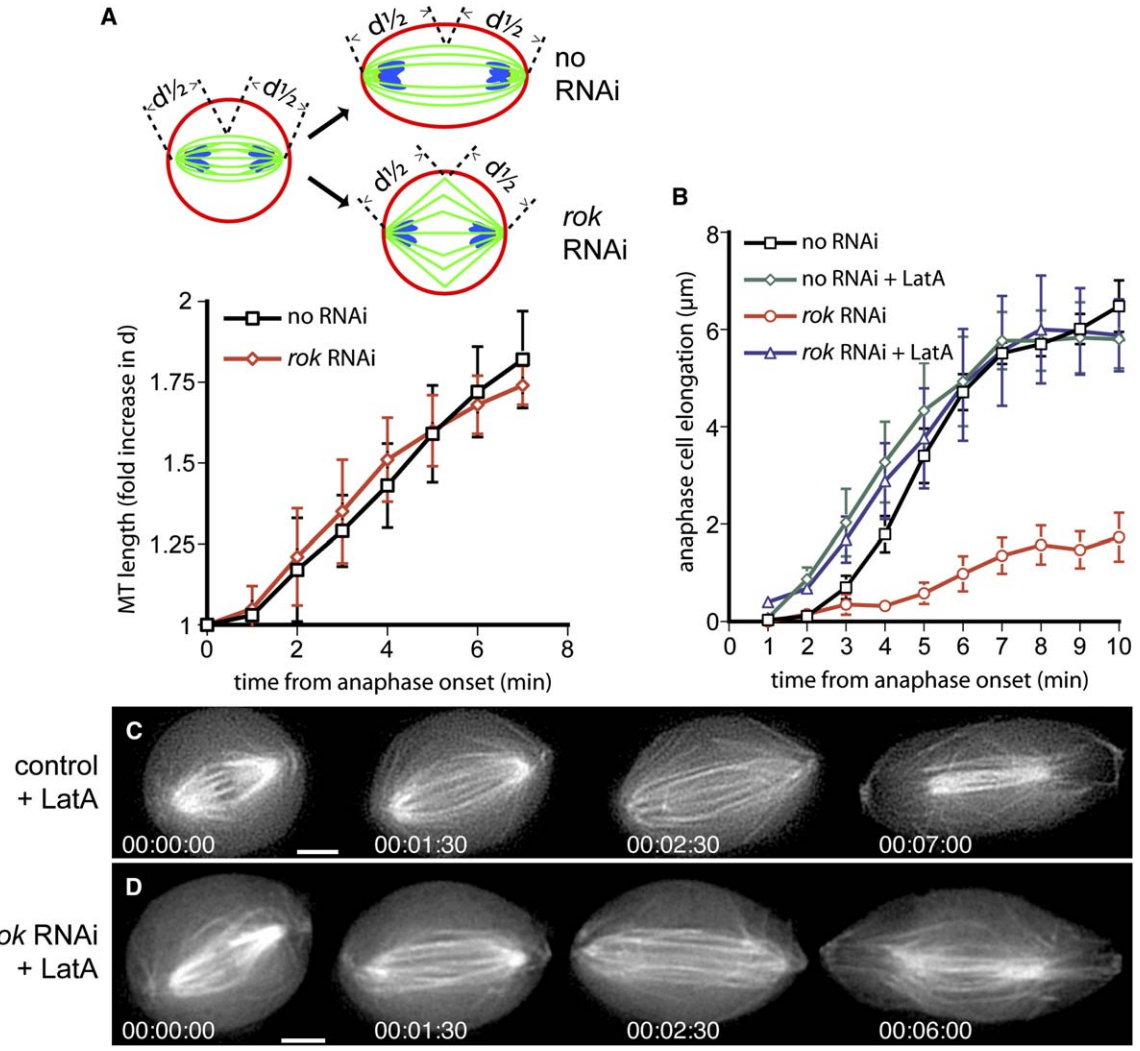

Figure 2. The Buckling of the Anaphase Spindle Following *rok* RNAi Depends on an Intact Actin Cortex

(A) Interpolar MT lengths (d) were determined from time-lapse sequences of individual GFP-tubulin-expressing cells with or without *rok* RNAi, as indicated in the cartoon. The fold increase in d over time from anaphase onset is plotted (mean ± standard deviation [SD], n = 5).

(B) Anaphase cell elongation (mean increase in cell length from metaphase ± standard error [SE], n = 5–12) was determined from time-lapse sequences of individual cells with or without *rok* RNAi in the presence or absence of Latrunculin A (LatA, 1 μg/ml, added 1–2 hr before imaging).

(C and D) Selected frames from representative time-lapse sequences in the presence of LatA (time from the metaphase/anaphase transition indicated in hr:min:s). (C) A control cell (see Movie 6). (D) A cell following 72 hr *rok* RNAi. Note how the morphology of the elongating spindle following rok RNAi closely resembles that of the control (see Movie 7). Scale bars represent 3 μm.

Spindles no longer showed any signs of buckling, and the central spindles formed at the normal location. Thus, Rok is not directly required for spindle elongation, at least under these circumstances. Furthermore, LatA-induced depolymerization of cortical actin bypasses the *rok* requirement for cell elongation. We conclude that the spindle collapse following *rok* RNAi depends on high cortical rigidity.

Myosin II, but Not Other Cytokinesis Functions, Is Also Required for Anaphase Cell Elongation

Nonmuscle myosin II is a regulatory target of Rok (reviewed in [16]). To follow the influence of Rok on the dynamics of myosin II recruitment to the cytokinetic furrow, we produced a stable S2 cell line expressing the *Drosophila* RLC, Spaghetti squash (Sqh), fused to GFP and under the control of the Sqh promoter [26, 27], as well as coexpressing an mRFP-tubulin fusion. In control metaphase cells, Sqh-GFP was diffusely localized in the cytoplasm, with only slight cortical enrichment (Figure 3A). Within 2–3 min of chromosome disjunction, a broad zone of Sqh-GFP accumulated at the equatorial cortex (Figure 3A, Movie 8). During elongation, this broad zone flattened, and furrows initiated from its center approximately 3–4 min after chromosome disjunction. In cells treated with *rok* dsRNA for 72–96 hr, this cortical accumulation of Sqh-GFP during anaphase was both delayed and reduced (Figures 3B and 3C and Movie 9). Despite this inhibition of equatorial Sqh-GFP recruitment, late furrows frequently formed in these

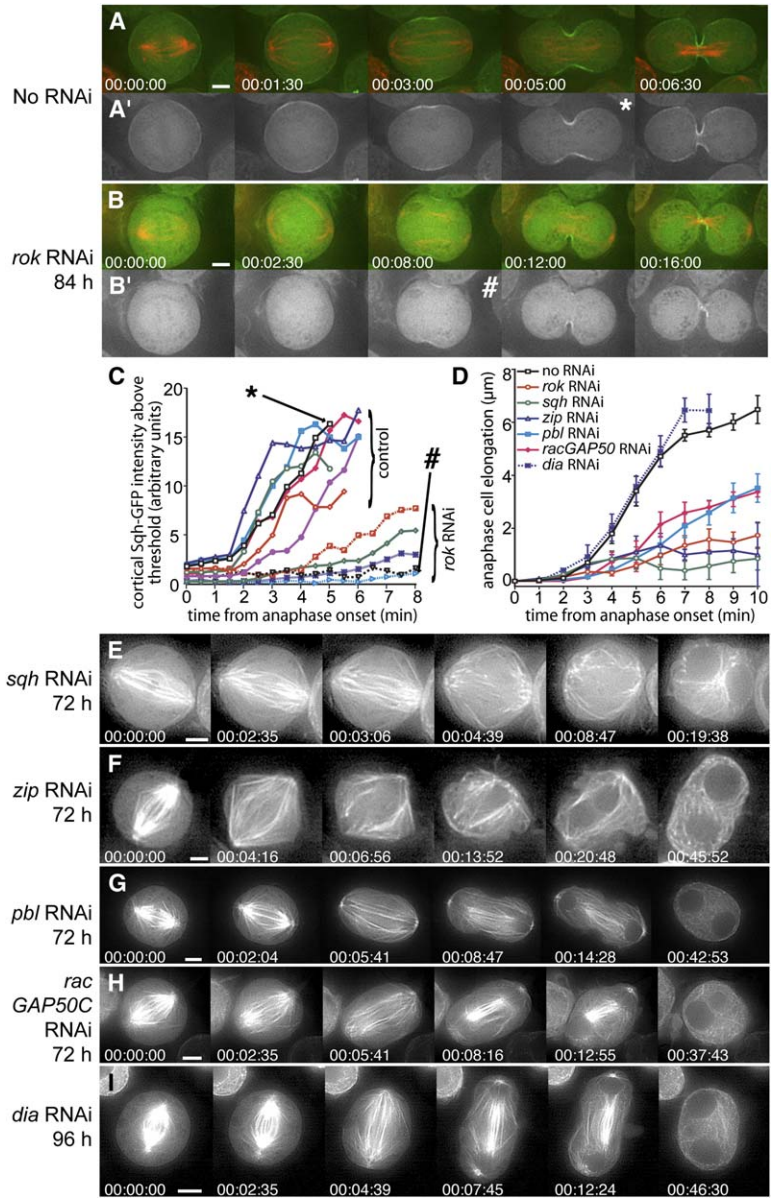

Figure 3. Anaphase Cell Elongation Requires Both *rok* and Myosin II Function, but Is Less Dependent on Other Cytokinesis Regulators

(A–B) Selected frames from time-lapse sequences of S2 cells expressing Spaghetti squash-GFP (in green and in [A′] and [B′]) and mRFP-tubulin (in red) and progressing through anaphase. (A) A control cell shows the rapid recruitment of Sqh-GFP to the equatorial cortex (see Movie 8). (B) Eighty-four hour *rok* RNAi caused a dramatic delay and reduction of cortical Sqh-GFP recruitment (Movie 9).

(C) Quantification of Sqh-GFP recruitment to the equatorial cortex in individual control and *rok* RNAi cells, performed as detailed in the Experimental Procedures. All of the *rok* RNAi cells ultimately furrowed, as in (B). Data points corresponding to the selected frames in A′ and B′ are indicated (*, #).

(D) Anaphase cell elongation (mean increase in cell length from metaphase ± SE, n = 3–9) was determined from time-lapse sequences of individual cells following the indicated RNAi treatments.

(E–I) Selected frames from time-lapse sequences of GFP-tubulin S2 cells. (E) Seventy-two hour *spaghetti squash* RNAi. The spindle buckled when the poles encountered the cortex, and cell elongation and cytokinesis failed (see Movie 10). (F) Seventy-two hour *zipper* (zip; myosin heavy chain) RNAi. Similarly, the spindle buckled as it tried to elongate in anaphase; cell elongation and cytokinesis both failed (00:13:52–00:20:48, see Movie 11). (G) Seventy-two hour *pebble* RNAi. Cell elongation occurred and a furrow initiated but then regressed (see Movie 12). (H) Seventy-two hour *RacGAP50C* RNAi. Some cell elongation occurred, but furrow ingression did not (see Movie 13). (I) Ninety-six hour *diaphanous* RNAi. Cell elongation occurred normally; a furrow initiated but then the cortex contracted wildly from side to side for several minutes before subsiding (see Movie 14). Times from the metaphase/anaphase transition are indicated in hr:min:s. Scale bars represent 3 μm.

Rok-depleted cells, and Sqh-GFP was present at the leading edge of these furrows, albeit at levels much reduced from normal (Figures 3B and 3C).

We also used immunofluorescence to examine the localization of the endogenous myosin II heavy chain, Zipper, in control and *rok*-dsRNA-treated S2 cells. *rok* RNAi led to a decrease in cortical Zipper accumulation in anaphase comparable to that observed with Sqh-GFP (Figure S1). We conclude that *rok* function is required for normal recruitment of myosin II to the cortex in anaphase.

These findings show that Rok activity influences myosin II very early in the progress toward cytokinesis. To test whether myosin II is required for cell elongation, we used RNAi to knock down *spaghetti squash* (*sqh*) or *zipper* and examined the effects on anaphase cell elongation in real time in GFP-tubulin S2 cells. RNAi of either of these genes led to a buckling of the spindle and a failure in cell elongation similar to that seen following *rok* RNAi (Figures 3E and 3F and Movies 10 and 11).

Because Pebble is thought to activate Rok and to initiate cytokinesis, we analyzed the *pebble* RNAi phenotype. Although a modest decrease in elongation was observed (Figure 3D), the dramatic spindle buckling did not occur: Instead, the major phenotype was a defect in furrowing (Figure 3G, Movie 12). Thus, Pebble makes a minor contribution to elongation and is essential for furrowing.

The Rho GTPase-activating protein RacGAP50C is thought to act cooperatively with Pebble in cytokinesis [28]. Just like *pebble* RNAi, *racGAP50C* RNAi caused mild reduction in elongation while severely compromising furrowing (Figures 3D and 3H, Movie 13).

Diaphanous, like Rok, is activated by Rho and is essential for cytokinesis [12]. *diaphanous* RNAi had no effect on anaphase cell elongation or spindle extension (Figures 3D and 3I). It did not block equatorial contraction either, but it prevented the formation of robust and stable cleavage furrows. Following normal initial contraction in the equatorial region, the contractile activity became highly unstable, migrating back and forth throughout the cortex rather than focusing at the equatorial midpoint to form a proper furrow (Figure 3I, Movie 14). These aberrant contractions subsided after several minutes, and any partial furrows that had formed regressed.

These findings indicate that anaphase cell elongation and cleavage-furrow ingression differ, at least in terms of the extent to which they are compromised by knockdown in the function of several genes that might otherwise be predicted to function in both processes. The finding that dsRNAs targeting *rok* or the regulatory target of Rok, myosin II, produced this unique phenotype whereas other dsRNAs did not argues that these functions have a specific role in promoting cell elongation.

Rok Promotes Furrowing

Thus far, we have emphasized the effects of Rok depletion on cell elongation. However, *rok* RNAi also delays furrow formation and slows its ingression. Consistent with previous demonstrations of increasing severity of RNAi phenotypes with the duration of RNAi [6], we saw increasingly severe defects in both cell elongation and furrowing with time of RNAi (Figures 1 and 4). After only 2–3 days of *rok* RNAi, neither elongation nor furrowing occurred at the normal time: The delay in elongation was sufficient to produce a penetrant spindle-buckling phenotype, but the cells did elongate in conjunction with late furrowing. Records taken at this stage showed successful albeit delayed division (Figure 4E and Movie 4, see also Figure 3B and Movie 9). Following more than 4 days of *rok* RNAi, we observed an accumulation of cells with two or more nuclei, suggesting a failure in cytokinesis (Figures 4A–4C). Real-time observations of cells after 4–5 days of RNAi treatment showed that cell elongation was severely affected and that many cells failed to furrow (Figure 4G and Movie 15). In cells that did initiate a furrow, the furrows appeared very late, and they ingressed slowly and often asymmetrically (Figure 4F and Movie 5). These furrows were also morphologically unusual: Rather than the normally valley-shaped furrow contour, the abnormal furrows had a steep canyon-like contour (Figure 4F). Despite such abnormalities, a defective cytokinesis such as that exhibited by the cell in Figure 4F would remarkably progress to the normal configuration of two daughter cells interconnected by an intercellular bridge. Importantly, the stability of these bridges was not compromised, unlike those that we previously described following depletion of the related Citron-kinase [6]. Thus, cytokinesis can sometimes succeed even after major physical disruptions induced by *rok* RNAi. Because late furrowing still occurred in some cells after prolonged *rok* RNAi, it might be argued that this type of furrowing is independent of Rok and that the cases of failure are secondary to earlier disruptions in the progress of mitosis and elongation. However, suppression of the furrowing defect by RNAi of an antagonist of Rok function (see below) suggests that a residual Rok-like activity does contribute to late furrowing. In summary, both elongation and furrowing are delayed early during *rok* RNAi treatment, whereas furrowing only fails completely later in the RNAi treatment.

Rho-kinase reportedly has a dual input in myosin II activation [16]. It stimulates myosin ATPase activity directly through activating phosphorylation of MRLC [13] and indirectly by inhibitory phosphorylation of the myosin binding subunit (Mbs), a protein that targets inhibitory phosphatase to myosin [20]. Because Rok and Mbs function antagonistically with respect to myosin function, we analyzed the effect of simultaneously depleting both gene products. *Mbs* RNAi substantially suppressed aspects of the *rok* RNAi phenotype. In particular, it dramatically suppressed the frequency of binucleate cells induced by *rok* RNAi (Figure 5A). Real-time analysis after prolonged exposure (7 days) to both dsRNAs showed that elongation was still perturbed (spindle buckling still occurred) but that the cells successfully divided (Figure 5B and Movie 16: also showing additional cells undergoing cytokinesis). Additionally, the furrows initiated late and ingressed slowly, suggesting that Rok plays a role in triggering cytokinesis at the time of its normal onset. Finally, the suppression of late furrowing failures upon *Mbs* RNAi suggests that cytokinesis failure after prolonged *rok* RNAi is due to a deficit in MRLC phosphorylation.

Given that MRLC phosphorylation is essential for myosin II function and cytokinesis [26], successful cytokinesis following double depletion of Rok and Mbs suggested that there might be alternative inputs into MRLC phosphorylation. For example, Citron kinase might provide a normally redundant contribution that is essential in this experimental context. This was a particularly attractive possibility given that Citron kinase, unlike Rok, lacks the ability to inhibit Mbs [15]. RNAi for all three genes–Rok, Mbs, and Citron kinase–gave a high frequency of multinucleate cells, indicating cytokinesis failure (Figure 5A). Remarkably, however, furrows still formed in the triply treated cells. Indeed, furrowing in these cells was indistinguishable from that seen in *rok* plus *Mbs* dsRNA-treated cells, arguing that Citron-kinase does not contribute importantly to furrowing. The triply treated cells exhibited the unstable intercellular bridge typical of the *citron kinase* RNAi phenotype, demonstrating that *citron kinase* function was compromised (Figure 5C, Movie 15). Our ability to recognize the distinct phenotypes of *rok* RNAi and *citron kinase* RNAi when these two dsRNAs are combined in the presence of Mbs dsRNA suggests that when Mbs is suppressed, these kinases have distinct functions and do not substantially modify each other's actions.

In an effort to identify potential contributions from other kinases known to possess MRLC kinase activity [16], we conducted similar triple RNAi experiments inactivating the candidate kinases in conjunction with RNAi of *rok* and *Mbs*. In this assay, RNAi to the myosin light-chain kinases *bent* and *stretchin-Mlck* and RNAi to the related kinases *genghis khan* (*gek*) and Pak-kinase (*Pak*) all failed to induce failures in cytokinesis when combined with *rok* and *Mbs* RNAi.

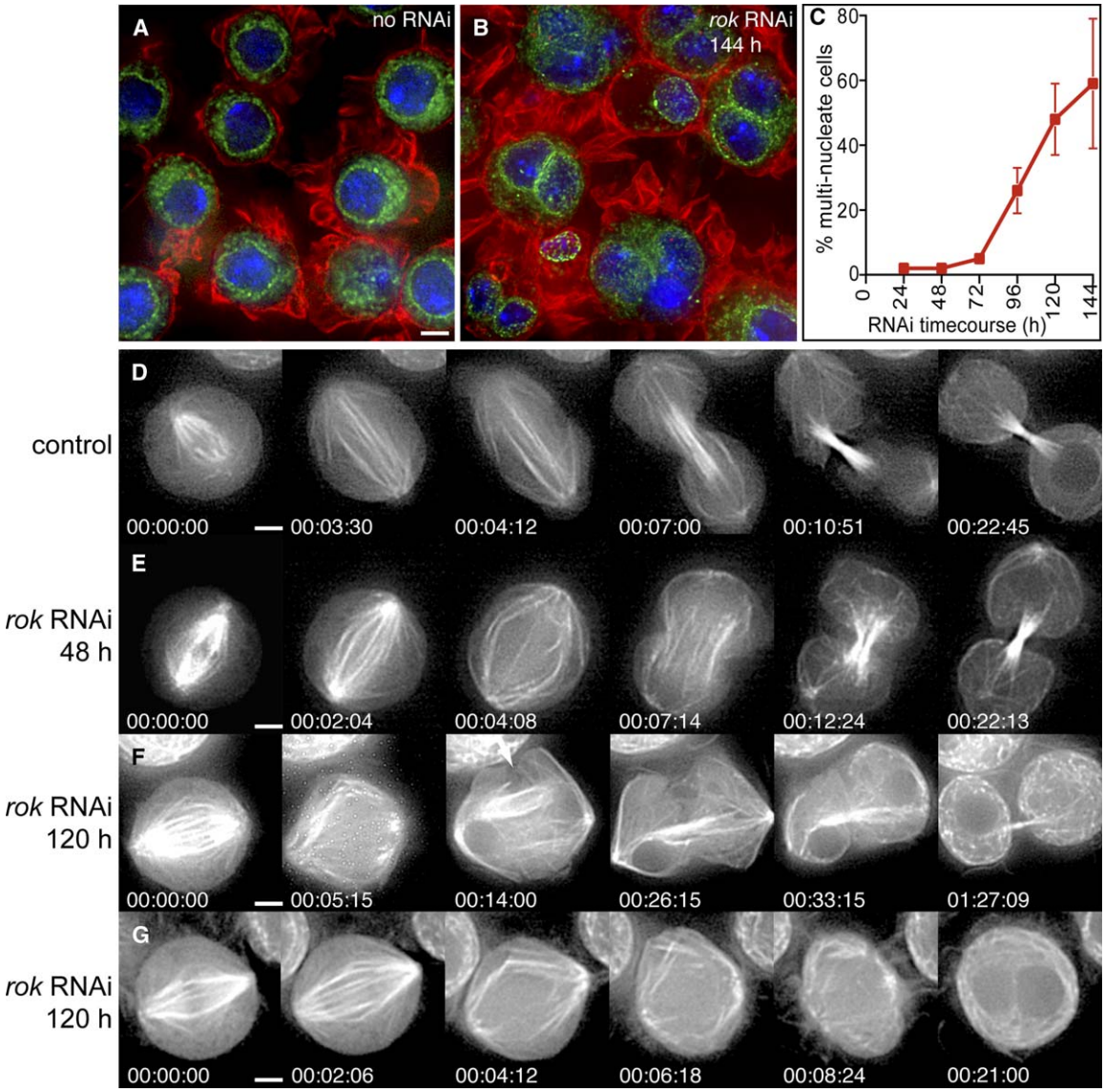

Figure 4. Contributions of Rok to Furrowing

(A and B) Fixed S2 cells stained for F-actin (phalloidin/red), nuclear envelope (wheat germ agglutinin/green), and DNA (Hoechst 33258/blue). (A) Control cells. (B) One hundred forty-four hour *rok* RNAi showing bi/multinucleate phenotype.

(C) Quantification of the incidence of bi/multinucleate cells as a function of duration of *rok* RNAi (mean ± SE, from three independent experiments).

(D–G) Selected frames from time-lapse sequences of GFP-tubulin S2 cells (time from the metaphase/anaphase transition indicated in hr:min:s). (D) Control cell undergoing cell elongation and cytokinesis (see Movie 3). (E) Cell following 48 hr *rok* RNAi. Cell elongation was delayed and reduced relative to mitotic progress, the spindle buckled, and the cell formed a robust cleavage furrow that was nonetheless delayed (see Movie 4). (F) Cell following 120 hr *rok* RNAi. Little or no cell elongation occurred, the spindle buckled, and after a large delay an asymmetric furrow formed and ingressed very slowly (arrow). Note the unusual shape of the furrow, which initiates as a narrow cleft rather than a smooth valley. Despite these abnormalities, cytokinesis succeeded (see Movie 5). (G) Cell following 120 hr *rok* RNAi. The buckling spindle was severely disrupted, and furrowing did not occur (see Movie 15). Note the cells depicted in (D)–(F) are the same as in Figures 1D–1F, but emphasizing later events. Scale bars represent 3 μm.

The results described in this section indicate that cytokinesis can occur despite major and early disruptions in cell elongation and spindle morphology, that Rok is needed for timely furrow ingression, and that even though Rok depletion can compromise the success of cytokinesis, suppression of *Mbs* allows Rok-depleted cells to divide successfully by using an abnormally late and slow furrowing process.

Discussion

How the complex events of mitosis and cytokinesis are seamlessly coordinated remains largely a mystery. Cell elongation is a characteristic feature linking mitosis and cytokinesis in many cell types [21, 22]. However, it has not been apparent how much attention this event deserves; it could be construed as a secondary

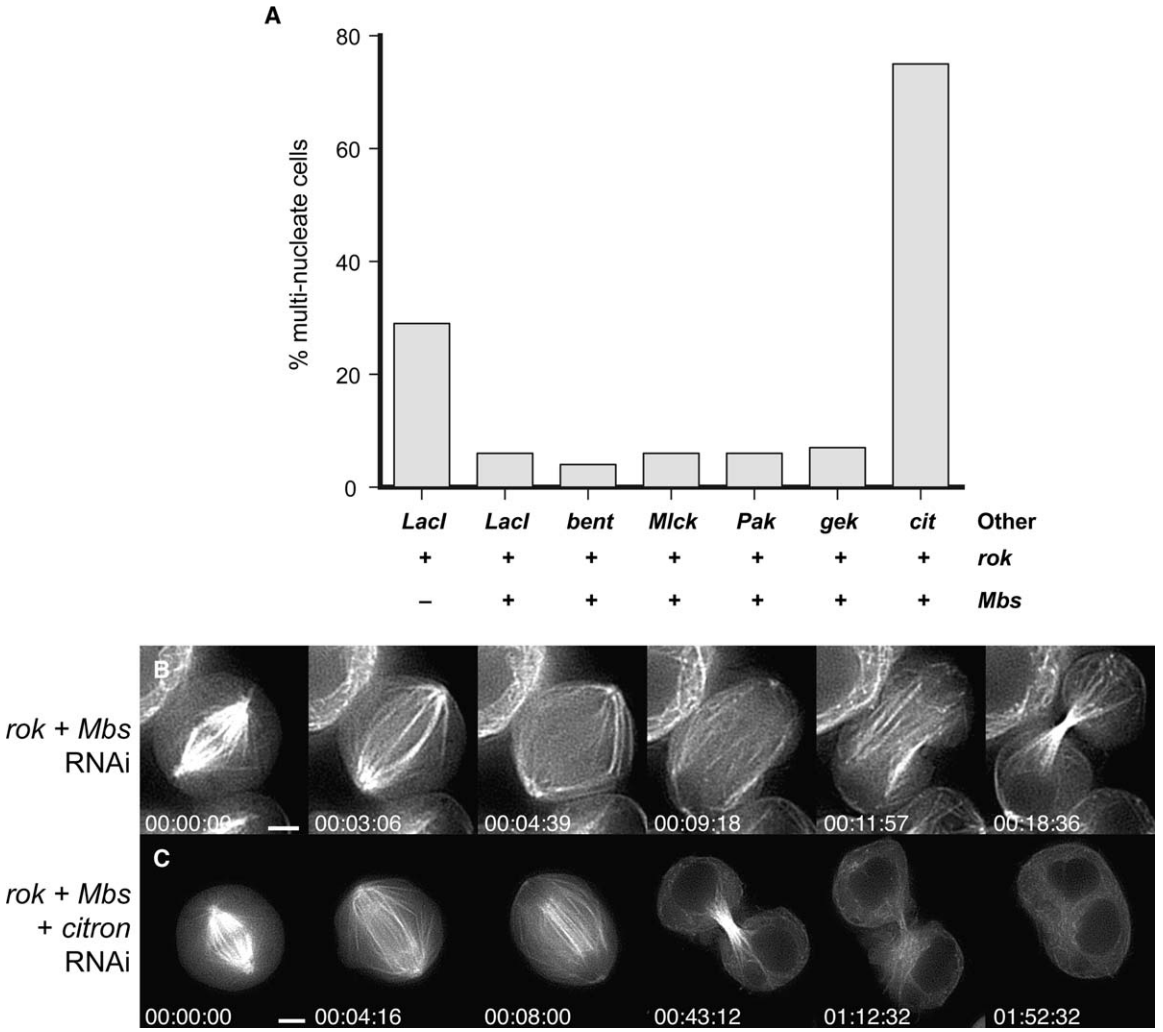

Figure 5. Other Potential MRLC Kinases Do Not Appear to Contribute Significantly to Furrowing

(A) Quantification of the incidence of bi/multinucleate cells induced by *rok* dsRNA in combination with a control dsRNA against *E. coli* LacI, or with further additions of *Mbs* dsRNA, which partially suppresses the *rok* RNAi phenotype, together with dsRNAs of other putative myosin RLC regulators: *bent* (Projectin myosin light chain kinase, CG32019); *Mlck* (*stretchin-MLCK*, CG18255); *Pak* (*PAK-kinase*, p21-activated kinase, CG10296); *gek* (*genghis khan*, Myotonic dystrophy kinase related, CG4012); and *cit* (*citron*, CG10522). S2 cells were incubated with equal amounts of dsRNA for 4 days, fixed, and stained, and the proportion of multinucleate cells counted. LacI dsRNA was used to standardize the total amounts of RNA added. *Mbs* RNAi greatly reduced the number of multinucleate cells induced by *rok* RNAi (compare first two bars). Except for *citron*, which is itself required for cytokinesis (see below), dsRNAs to other putative MRLC kinases had no effect on the frequency of failed cytokinesis in cells depleted of Rok and Mbs.

(B–C) Selected frames from time-lapse sequences of GFP-tubulin S2 cells. (B) A cell following 7 days *rok* + *Mbs* RNAi. Cell elongation was perturbed (note the buckled spindle 00:04:39), and furrowing was delayed and slowed, but cytokinesis was successful (see Movie 16). (C) A cell following 4 days *rok* + *Mbs* + *cit* RNAi. As with *rok* + *Mbs* RNAi, furrowing was delayed and slowed but nonetheless successful. However, cytokinesis still failed through instability of the intercellular bridge, the phenotype characteristic of *citron* RNAi alone (see Movie 17).

consequence of spindle extension or an early manifestation of the gradual recruitment of contractile elements that form the contractile ring. Our results suggest that, although it is inextricably linked with both mitosis and cytokinesis, there are distinctive genetic contributions to its success (see below).

One of our most striking findings was that depletion of *rok* function prevented anaphase cell elongation and caused a dramatic buckling of the spindle. Taking many observations into account, we infer that the primary defect was one where the cortex failed to respond appropriately and, as a result, the spindle suffered a mechanical disruption as it encountered the unresponsive cortex. Thus, *rok* is required for remodeling the cell cortex during anaphase cell elongation, and perturbation of *rok* function disrupts the normal temporal coordination of cortex and spindle. In this regard, Rok might be required for the spindle to communicate with the cortex to stimulate elongation, or it might simply be required to execute elongation. In either case, the anaphase spindle extension alone is clearly insufficient to push the sides of the cell out and promote cell elongation. In addition, continued spindle elongation within the restricted confines of the rigid cortex demonstrates that there is no

feedback signal from the cortex to the spindle. Thus, cell elongation and spindle extension are likely coupled only in a unidirectional manner: The cortex responds to the growing spindle, but the spindle does not sense an unyielding cortex. To our knowledge, these important conclusions have not previously been drawn.

Our data also clearly indicate that Rok is required for normal myosin II recruitment to the equatorial cortex, a finding also recently reported by others [29], and one that has been previously suggested by using a pharmacological inhibitor of mammalian Rho-kinase [30]. We have found that myosin II is also required for cell elongation, suggesting that it is the relevant target of Rok action. In this regard, we note that a similar failure of cell elongation was observed in the neuroblasts of *Drosophila* larvae homozygous for *sqh*^{1}, a hypomorphic *spaghetti squash* allele [31]. Although not specifically commented on in the paper describing this mutant, the figures show poorly elongated anaphase and telophase cells in which the segregated DNA masses were in tight apposition with the cell cortex [31]. The similarity between those phenotypes and the ones we describe here in S2 cells strongly suggests that a similar Rok/myosin II pathway operates in vivo in the developing fly.

Genetic-interaction studies have demonstrated that *rok* functions in the Pebble pathway to influence cytokinesis in the wing disc [1]. However, *rok* mutant cells can divide at least several times to produce a substantial clone in the wing disc [32]. Although this latter finding may lead one to question the importance of *rok* in cytokinesis, apparent dispensability in this context should not be taken as a lack of importance. Continued division of S2 cells with compromised *rok* function occurs in the face of major perturbations, and, after prolonged *rok* RNAi, we and another recent study [29] document frequent failures in cytokinesis. We suggest that *rok* plays an integral part in promoting and coordinating cytokinesis and that successful cytokinesis with compromised *rok* function is testament to the robustness of the process.

Given that cytokinesis is so robust, a consideration of how loss of *rok* function alters the normal progression of the process might provide more insight than a consideration of its overall success. In addition to the extreme defect in which furrowing is blocked, *rok* RNAi causes a pronounced delay in the onset of furrowing and reduction in the rate of ingression of furrows. Simultaneous depletion of Mbs prevented failures in cytokinesis but did not restore the normal timing of furrowing. Thus, Rok promotes whereas Mbs suppresses furrow ingression. Additionally, the normal timing requires Rok, indicating that its activity contributes to triggering the onset of furrowing. Studies in *C. elegans* have also found that Let-502 (the Rok ortholog) and MEL-11 (the Mbs ortholog) play antagonistic roles in furrow ingression, but in contrast to our observations in S2 cells, in *C. elegans*, the activity of Let-502 appeared to control the speed of ingression without influencing the timing of onset of furrowing [33].

Among the cytokinesis genes that we examined, only RNAi of *rok* and myosin II gave a severe block to elongation, and, in the case of *rok*, this often gave a strong elongation effect without blocking furrowing. We also found that RNAi of *pebble* and *racGAP50c* slowed elongation to half its normal rate while severely suppressing furrowing. RNAi of other cytokinesis genes, such as *diaphanous*, *citron kinase*, and *anillin*, did not interfere with elongation (Figure 3, [6], and data not shown). Given these findings, we suggest that elongation and furrowing, although they share some common functions, are differentially regulated and ought to be recognized as distinct subroutines in the overall process of cytokinesis. Given that Pebble is an upstream activator of Rho and Rok in cytokinesis, the finding that *pebble* RNAi gave a more mild elongation defect suggests that a different Rok activator promotes elongation: For example, Rok might be activated by other Rho-GEFs, as it is in interphase.

Two processes likely contribute to cell elongation—equatorial contraction and polar relaxation—and this duality may contribute to some of the apparent overlap in the regulation of elongation and furrowing. Rok mediated equatorial recruitment and activation of myosin II might contribute to equatorial contraction and provide one input into elongation. This input is likely to depend on Pebble and RacGAP50C which also localize to the equator and are known to influence Rho function. The partial defect in cell elongation induced by *pebble* or *racGAP50c* RNAi might be explained by disruption of this contraction. Other indications suggest that polar relaxation occurs in S2 cell cytokinesis and that *rok* RNAi interferes with the process. During elongation, the polar cortices bleb and appear to be actively remodeled as if signaled to do so by the approaching spindle poles, whereas following *rok* RNAi the segregating spindle poles push right up against the cortex. We also note that mitotic spindle poles have been shown in other systems to harbor active Rho (as evidenced through a GFP-Rho binding domain reporter [34]), Rho-kinase [35] and myosin II regulatory light chains phosphorylated on the Rho-kinase phosphorylation site [36]. In addition, mammalian ROCKI/II are responsible for membrane blebbing during apoptosis and therefore clearly able to promote such an outcome [37, 38]. Thus, it is not inconceivable that a Rok/myosin II pathway could operate at the spindle poles during anaphase to promote polar relaxation. We suspect that Rok and myosin II function in two pathways, one governing equatorial contraction and the other polar relaxation, either of which can support cell elongation, whereas Pebble and RacGap50C interfere only with cortical contraction and hence result in a partial elongation defect (Figure 6).

It seems likely that some divisions, particularly those that are asymmetric, might be particularly dependent on polar relaxation and hence be more sensitive to *rok* depletion than others. For example, asymmetric divisions might rely on differential actions at the spindle poles. Indeed, the sensitivity of the initial stages of polar-body formation in mouse eggs to an inhibitor of the mammalian Rok suggests that Rok may play a role in the formation of the cortical protrusion into which the spindle migrates in this highly asymmetric division [39].

Conclusions

In summary, we have uncovered pivotal roles for Rok in the earliest shape change of cytokinesis: anaphase cell elongation. Our model of cell elongation and the onset of cytokinesis is depicted in Figure 6. As the spindle

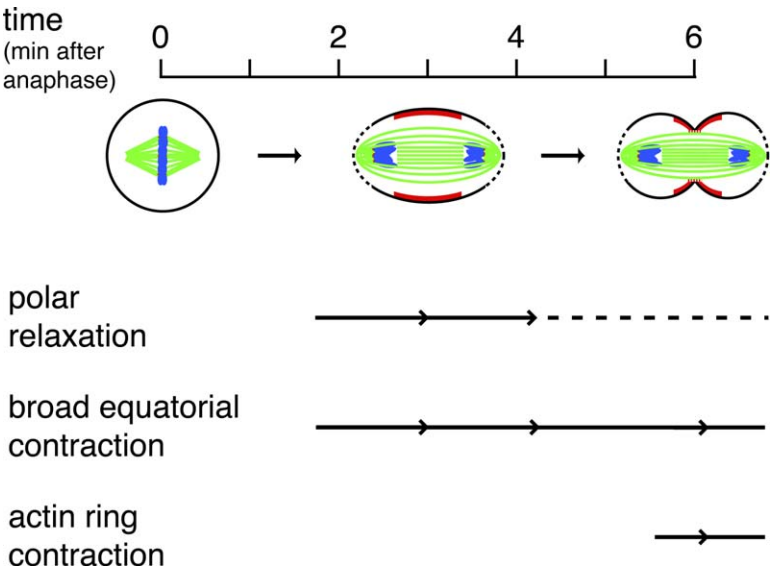

Figure 6. Model for Anaphase Cell Elongation and Initiation of Cytokinesis in *Drosophila* S2 Cells

We propose that both polar relaxation and equatorial contraction contribute to anaphase cell elongation and the initiation of cytokinesis in S2 cells. In our model, the cell undergoes the transition to anaphase with the rigid cortex of a metaphase cell (in black), but this rigidity must be modulated during anaphase. As the chromosomes (in blue) segregate and the anaphase spindle (MTs in green) extends, the polar cortices relax (dotted lines) and a broad contraction begins at the cell equator (in red). Both of these processes, which normally occur around 2–3 min from anaphase onset, require Rok (and Myosin II): As a result, elongation is effectively blocked by depletion of Rok. In contrast, Pebble and RacGAP50C only have an input into the broad equatorial contraction so that depletion does not remove the polar relaxation input into cell elongation. Later, around 5 min after anaphase onset, an actin ring (dotted red line) drives furrow ingression from the center of the earlier broad zone of contractility. Actin ring contraction is sensitive to Pebble, RacGAP50C, and Diaphanous depletion, but Rok depletion, unless severe or prolonged, leads only to a delay in furrowing and modification of the shape of the ingressing furrow. We propose that all three processes of polar relaxation, broad equatorial contraction, and actin ring contraction are promoted by Rok and myosin II, whereas other cytokinesis regulators such as Pebble are more specialized in the promotion of equatorial contraction and actin ring assembly. Accordingly, Rok depletion is particularly effective at blocking/delaying the earliest events in cytokinesis.

extends in anaphase B, Rok stimulates polar relaxation, allowing the spindle to push the sides of the cell out as it extends. In addition, Rok stimulates myosin II recruitment to the equatorial cortex, where it begins to contract in a broad zone. At the center of this broad zone, the contractile actin ring then forms and the cytokinetic furrow ingresses. Distinctions in gene requirements for anaphase cell elongation versus furrowing suggest distinctions between the two processes.

It is intriguing that Rok and/or myosin II appears to be involved in the whole gamut of cell shape changes that occur during cell division: mitotic cell rounding [10], anaphase cell elongation (this study), cytokinetic furrowing (see [16]), and postmitotic spreading [40]. This implies that the same fundamental machinery mediates each of these dramatic cytoskeletal rearrangements. Understanding how these events are regulated so as to ensure the appropriate response at the appropriate time is one of the challenges ahead.

Experimental Procedures

Materials

Latrunculin A was purchased from Calbiochem; Alexa^{488}- and Alexa^{546}-conjugated secondary antibodies and rhodamine-phalloidin were from Molecular Probes. Rabbit polyclonal anti-Zipper antibody was from Dr. Kiehart (used 1:500), and monoclonal anti-α-tubulin was from Sigma.

Cell Lines, Cell Culture, and RNAi

Histone H2B-GFP was excised from the pEGFP-N1 plasmid described in [41] and subcloned into pAc5.1 (Invitrogen). This was then cotransfected into *Drosophila* S2 cells with pCoHygro and selected for with standard procedures (Invitrogen). The GFP-tubulin cells have been previously described [23]. The Spaghetti squash-GFP cells were produced by cotransfection of the plasmid described in [27] with one encoding mRFP-tubulin in pMT (kindly provided by Patrick Heun) and pCoHygro and selected for with standard procedures. Prior to imaging, mRFP-tubulin expression was induced by overnight incubation with 400 μM $CuSO_4$.

Cells were cultured in glass-bottomed imaging 96-well plates (BD Falcon, ref 357311), as described in [6]. dsRNAs were produced as described in [6], with the primer sequences detailed in the Supplemental Data. Two independent *rok* dsRNAs produced comparable phenotypes, and incubation of cells with either *rok* dsRNA reduced the level of the endogenous *rok* mRNA, as evidenced by real-time RT-PCR analysis (data not shown).

Image Acquisition and Analysis

For time-lapse video microscopy, cells were imaged at room temperature (RT) directly in the 96-well glass-bottomed culture plates with an Olympus 1X70 inverted microscope with a 100× objective (numerical aperture 1.4), with single Z sections (0.5–1 s exposures) taken every 20–60 s. The resulting datasets were deconvolved and converted to Quicktime format with Deltavision software (IVE/Priism 4.2.0). For fixed-cell microscopy, the same setup was used, although Z series (0.2 μm sections) were taken and deconvolved, and partial projections were manipulated in Adobe Photoshop 8.0. Distance measurements and quantification of intensities were performed with Priism software. Quantification of Sqh-GFP recruitment to the equatorial cortex was performed as follows: The mean pixel intensity of Sqh-GFP was determined for each cell in metaphase and used as a threshold value for the subsequent time-lapse series. The total intensities above this threshold were then measured for both sides of the equatorial cortex visible in the cross-sectional view of the cell at each time point in the series. The means of the two values were then plotted against time.

Supplemental Data

Supplemental Data include Supplemental Experimental Procedures, one figure, and seventeen movies and are available with this article online at: http://www.current-biology.com/cgi/content/full/16/4/359/DC1/.

Acknowledgments

We thank Devin Parry and Raphael Buencamino for creating the histone H2B-GFP S2 cell line, Patrick Heun for creating the mRFP-

tubulin pMT construct, and Roger Tsien for providing the mRFP. We also thank Eric Branlund for help with IVE/Priism software and David Morgan, Mark McCleland, Tony Shermoen, Soo-Jung Lee, Catherine Sheppard, and Reed Kelso for comments on the manuscript. A.E. thanks the Association pour la Recherche sur le Cancer (ARC grant 3269). This research was supported by a grant from the Susan G. Komen Breast Cancer Foundation (postdoctoral fellowship to G.R.X.H.) and by National Institutes of Health grants GM37193 and GM60988 to P.H.O'F.

Received: September 7, 2005
Revised: December 23, 2005
Accepted: December 29, 2005
Published: February 21, 2006

References

1. Echard, A., and O'Farrell, P.H. (2003). The degradation of two mitotic cyclins contributes to the timing of cytokinesis. Curr. Biol. *13*, 373–383.
2. Mishima, M., Pavicic, V., Gruneberg, U., Nigg, E.A., and Glotzer, M. (2004). Cell cycle regulation of central spindle assembly. Nature *430*, 908–913.
3. Glotzer, M. (2001). Animal cell cytokinesis. Annu. Rev. Cell Dev. Biol. *17*, 351–386.
4. Glotzer, M. (2005). The molecular requirements for cytokinesis. Science *307*, 1735–1739.
5. Guertin, D.A., Trautmann, S., and McCollum, D. (2002). Cytokinesis in eukaryotes. Microbiol. Mol. Biol. Rev. *66*, 155–178.
6. Echard, A., Hickson, G.R., Foley, E., and O'Farrell, P.H. (2004). Terminal cytokinesis events uncovered after an RNAi screen. Curr. Biol. *14*, 1685–1693.
7. Eggert, U.S., Kiger, A.A., Richter, C., Perlman, Z.E., Perrimon, N., Mitchison, T.J., and Field, C.M. (2004). Parallel chemical genetic and genome-wide RNAi screens identify cytokinesis inhibitors and targets. PLoS Biol. *2*, e379.
8. Somma, M.P., Fasulo, B., Cenci, G., Cundari, E., and Gatti, M. (2002). Molecular dissection of cytokinesis by RNA interference in Drosophila cultured cells. Mol. Biol. Cell *13*, 2448–2460.
9. Matzke, R., Jacobson, K., and Radmacher, M. (2001). Direct, high-resolution measurement of furrow stiffening during division of adherent cells. Nat. Cell Biol. *3*, 607–610.
10. Maddox, A.S., and Burridge, K. (2003). RhoA is required for cortical retraction and rigidity during mitotic cell rounding. J. Cell Biol. *160*, 255–265.
11. Prokopenko, S.N., Brumby, A., O'Keefe, L., Prior, L., He, Y., Saint, R., and Bellen, H.J. (1999). A putative exchange factor for Rho1 GTPase is required for initiation of cytokinesis in Drosophila. Genes Dev. *13*, 2301–2314.
12. Castrillon, D.H., and Wasserman, S.A. (1994). Diaphanous is required for cytokinesis in Drosophila and shares domains of similarity with the products of the limb deformity gene. Development *120*, 3367–3377.
13. Amano, M., Ito, M., Kimura, K., Fukata, Y., Chihara, K., Nakano, T., Matsuura, Y., and Kaibuchi, K. (1996). Phosphorylation and activation of myosin by Rho-associated kinase (Rho-kinase). J. Biol. Chem. *271*, 20246–20249.
14. Kosako, H., Yoshida, T., Matsumura, F., Ishizaki, T., Narumiya, S., and Inagaki, M. (2000). Rho-kinase/ROCK is involved in cytokinesis through the phosphorylation of myosin light chain and not ezrin/radixin/moesin proteins at the cleavage furrow. Oncogene *19*, 6059–6064.
15. Yamashiro, S., Totsukawa, G., Yamakita, Y., Sasaki, Y., Madaule, P., Ishizaki, T., Narumiya, S., and Matsumura, F. (2003). Citron kinase, a Rho-dependent kinase, induces di-phosphorylation of regulatory light chain of myosin II. Mol. Biol. Cell *14*, 1745–1756.
16. Matsumura, F. (2005). Regulation of myosin II during cytokinesis in higher eukaryotes. Trends Cell Biol. *15*, 371–377.
17. Shandala, T., Gregory, S.L., Dalton, H.E., Smallhorn, M., and Saint, R. (2004). Citron kinase is an essential effector of the Pbl-activated Rho signalling pathway in Drosophila melanogaster. Development *131*, 5053–5063.
18. D'Avino, P.P., Savoian, M.S., and Glover, D.M. (2004). Mutations in sticky lead to defective organization of the contractile ring during cytokinesis and are enhanced by Rho and suppressed by Rac. J. Cell Biol. *166*, 61–71.
19. Naim, V., Imarisio, S., Di Cunto, F., Gatti, M., and Bonaccorsi, S. (2004). Drosophila citron kinase is required for the final steps of cytokinesis. Mol. Biol. Cell *15*, 5053–5063.
20. Kawano, Y., Fukata, Y., Oshiro, N., Amano, M., Nakamura, T., Ito, M., Matsumura, F., Inagaki, M., and Kaibuchi, K. (1999). Phosphorylation of myosin-binding subunit (MBS) of myosin phosphatase by Rho-kinase in vivo. J. Cell Biol. *147*, 1023–1038.
21. Rappaport, R. (1996). Cytokinesis in Animal Cells (Cambridge: Cambridge University Press).
22. Wilson, E. (1925). The Cell in Development and Heredity, Third Edition (New York: The Macmillan Company).
23. Goshima, G., and Vale, R.D. (2003). The roles of microtubule-based motor proteins in mitosis: Comprehensive RNAi analysis in the Drosophila S2 cell line. J. Cell Biol. *162*, 1003–1016.
24. Petersen, N.O., McConnaughey, W.B., and Elson, E.L. (1982). Dependence of locally measured cellular deformability on position on the cell, temperature, and cytochalasin B. Proc. Natl. Acad. Sci. USA *79*, 5327–5331.
25. Wakatsuki, T., Schwab, B., Thompson, N.C., and Elson, E.L. (2001). Effects of cytochalasin D and latrunculin B on mechanical properties of cells. J. Cell Sci. *114*, 1025–1036.
26. Jordan, P., and Karess, R. (1997). Myosin light chain-activating phosphorylation sites are required for oogenesis in Drosophila. J. Cell Biol. *139*, 1805–1819.
27. Rogers, S.L., Wiedemann, U., Hacker, U., Turck, C., and Vale, R.D. (2004). Drosophila RhoGEF2 associates with microtubule plus ends in an EB1-dependent manner. Curr. Biol. *14*, 1827–1833.
28. Somers, W.G., and Saint, R. (2003). A RhoGEF and Rho family GTPase-activating protein complex links the contractile ring to cortical microtubules at the onset of cytokinesis. Dev. Cell *4*, 29–39.
29. Dean, S.O., Rogers, S.L., Stuurman, N., Vale, R.D., and Spudich, J.A. (2005). Distinct pathways control recruitment and maintenance of myosin II at the cleavage furrow during cytokinesis. Proc. Natl. Acad. Sci. USA *102*, 13473–13478.
30. Straight, A.F., Cheung, A., Limouze, J., Chen, I., Westwood, N.J., Sellers, J.R., and Mitchison, T.J. (2003). Dissecting temporal and spatial control of cytokinesis with a myosin II Inhibitor. Science *299*, 1743–1747.
31. Karess, R.E., Chang, X.J., Edwards, K.A., Kulkarni, S., Aguilera, I., and Kiehart, D.P. (1991). The regulatory light chain of nonmuscle myosin is encoded by spaghetti-squash, a gene required for cytokinesis in Drosophila. Cell *65*, 1177–1189.
32. Winter, C.G., Wang, B., Ballew, A., Royou, A., Karess, R., Axelrod, J.D., and Luo, L. (2001). Drosophila Rho-associated kinase (Drok) links Frizzled-mediated planar cell polarity signaling to the actin cytoskeleton. Cell *105*, 81–91.
33. Piekny, A.J., and Mains, P.E. (2002). Rho-binding kinase (LET-502) and myosin phosphatase (MEL-11) regulate cytokinesis in the early Caenorhabditis elegans embryo. J. Cell Sci. *115*, 2271–2282.
34. Bement, W.M., Benink, H.A., and von Dassow, G. (2005). A microtubule-dependent zone of active RhoA during cleavage plane specification. J. Cell Biol. *170*, 91–101.
35. Chevrier, V., Piel, M., Collomb, N., Saoudi, Y., Frank, R., Paintrand, M., Narumiya, S., Bornens, M., and Job, D. (2002). The Rho-associated protein kinase p160ROCK is required for centrosome positioning. J. Cell Biol. *157*, 807–817.
36. Matsumura, F., Ono, S., Yamakita, Y., Totsukawa, G., and Yamashiro, S. (1998). Specific localization of serine 19 phosphorylated myosin II during cell locomotion and mitosis of cultured cells. J. Cell Biol. *140*, 119–129.
37. Sebbagh, M., Hamelin, J., Bertoglio, J., Solary, E., and Breard, J. (2005). Direct cleavage of ROCK II by granzyme B induces target cell membrane blebbing in a caspase-independent manner. J. Exp. Med. *201*, 465–471.
38. Coleman, M.L., Sahai, E.A., Yeo, M., Bosch, M., Dewar, A., and Olson, M.F. (2001). Membrane blebbing during apoptosis results

from caspase-mediated activation of ROCK I. Nat. Cell Biol. *3*, 339–345.

39. Zhong, Z.S., Huo, L.J., Liang, C.G., Chen, D.Y., and Sun, Q.Y. (2005). Small GTPase RhoA is required for ooplasmic segregation and spindle rotation, but not for spindle organization and chromosome separation during mouse oocyte maturation, fertilization, and early cleavage. Mol. Reprod. Dev. *71*, 256–261.
40. Cramer, L.P., and Mitchison, T.J. (1995). Myosin is involved in postmitotic cell spreading. J. Cell Biol. *131*, 179–189.
41. Kanda, T., Sullivan, K.F., and Wahl, G.M. (1998). Histone-GFP fusion protein enables sensitive analysis of chromosome dynamics in living mammalian cells. Curr. Biol. *8*, 377–385.